Journal of Fluorescence (2018) 28:639–653
https://doi.org/10.1007/s10895-018-2226-3

ORIGINAL ARTICLE

Red Emitting Monoazo Disperse Dyes with Phenyl(1H-benzoimidazol-5-yl) Methanone as Inbuilt Photostabilizing Unit: Synthesis, Spectroscopic, Dyeing and DFT Studies

Amol G. Jadhav[1] · Suvidha S. Shinde[1] · Nagaiyan Sekar[1]

Received: 6 February 2018 / Accepted: 27 March 2018 / Published online: 4 April 2018

Abstract

Synthesis of three novel phenyl(1H-benzoimidazol-5-yl)methanone based fluorescent monoazo disperse dyes and their characterization by spectroscopic methods (^{1}H NMR, ^{13}C NMR, IR and MS) are presented. Insertion of phenyl(1H-benzoimidazol-5-yl)methanone moiety bring about induced fluorescence properties and enhanced photostability as compared to the previously reported analogues (**CI Solvent Yellow 14**, **4-diethylamino-2-hydroxy-1-diazobenzene** and **7-(diethylamino)-4-hydroxy-3-(phenyldiazenyl)-2H-chromen-2-one)**. Synthesized phenyl(1H-benzoimidazol-5-yl)methanone based dyes exhibited red-shifted absorption maxima (497–516 nm), high molar extinction coefficients and are emitting in the far-red region (565–627 nm). Moreover, naphthalene-comprising dyes showed negative solvatochromism while *N,N*-diethylamine comprising dyes showed positive solvatochromism and are in good agreement with solvent polarity graphs and the computed energy levels of highest occupied and lowest unoccupied molecular orbitals. Synthesised dyes have better photostability (light fastness) and sublimation fastness on dyed polyester and nylon compared to reported analogues**.** DFT calculated energies, electrophilicity index and Frontier Molecular Orbitals (FMO's) enabled to evaluate the stabilities of azo and hydrazone forms of the dyes.

Keywords Phenyl(1H-benzoimidazol-5-yl)methanone · Fluorescent monoazo dyes · Solvatochromism · Aza-hydrazone and DFT study

Introduction

Azo dyes cover the single largest group of dyes with respect to number and production scales with many industrial applications to introduce new and efficient colours to the substrates [1]. They are most versatile and robust having high tinctorial strengths with a full-color range from yellow to blue-green shades [2]. The high molar extinction coefficient, structural diversity, good fastness properties and ease of synthesis have made these dyes very successful [3–5]. Economy and ease of preparation of azo dyes have made them highly applicable to many colour industries [6, 7]. But fastness improvements are vital in the textile industry since dyed fabrics have found wide applications and are exposed to direct sunlight [8].

Benzophenone based dyes have found applications in photoinitiators and photosensitizers [9], thermal stabilizers [10], UV absorbers [11], oxidants in photo-induced electron transfer (PET) [12], fluorescent chemosensors [13], biological probes [14] and Excites State Intramolecular Proton Transfer (ESIPT) based fluorescent chemosensors [15, 16]. In general, benzophenone unit is photostabilizing and UV blocking entity [17]. Stability is influenced by appropriate substitutions in the aromatic ring at various positions of benzophenone [18]. Substitution at meta-position to the carbonyl group of benzophenone derivatives show good intramolecular redox process [19]. Similarly, substitution at para-position remarkably modifies photochemistry of the molecule [20]. Such appropriately modified few promising benzophenone based mordant and acid azo dyes are available in the literature [21, 22]. Some of

Amol G. Jadhav and Suvidha S. Shinde contributed equally to this work.

Electronic supplementary material The online version of this article (https://doi.org/10.1007/s10895-018-2226-3) contains supplementary material, which is available to authorized users.

✉ Nagaiyan Sekar
n.sekar@ictmumbai.edu.in; nethi.sekar@gmail.com

[1] Department of Dyestuff Technology, Institute of Chemical Technology, Nathalal Parekh Marg, Matunga, Mumbai 400 019, India

the reported benzophenone derivatives are emissive [23–26]. In the same line Barsotti et al. recently did extensive studies on fluorescence properties of 4-hydroxy benzophenone [23, 27].

Similarly, dyes containing imidazole unit have found wide applications in dye sensitizer solar cells (DSSC) [28], hole transporting materials [29], ESIPT based dyes [30] fluorescent sensor [31] and solid-state emissive dyes [32]. Dyes with imidazole unit are also used in singlet oxygen generation [33] and radical photopolymerization reactions [34]. Due to strong accepting capacity [35] and high molar extinction coefficients [36] of imidazole-based dyes, photostability gets enhanced [37].

An important use of fluorescent dyestuffs is in the coloration of synthetic fibres like polyesters, acrylics and polyamides. Fluorescent textiles not only increases visibility but also provides high design options [38]. Many dyes for acrylic fibres, particularly methines such as CI Basic Violet 7, CI Basic Red 13 and CI Basic Red 74 are fluorescent and very bright resulting into important fluorescent textile fibres [38]. The dominating structural classes for fluorescent textiles dyes include coumarins, perylene and methines [38, 39]. But the available dyes do not meet the simultaneous requirement of both good fluorescent properties and light fastness properties. So, in order to develop synthetic dyes for textile applications, it is advisable that modern colourants should have both photostabilities as well as improved spectroscopic characteristics [40].

Considering combined advantages of both benzophenone core and imidazole unit we developed in-built stabilising phenyl(1H-benzo[d]imidazol-5-yl)methanone group. Presence of donors (–$N(Et)_2$, -OH groups), acceptors (imidazole, >C=O) and long π-conjugation [41] in the present phenyl(1H-benzo[d]imidazol-5-yl)methanone based azo dyes enable them to act as good candidates for attractive fluorescent compounds. However, very few reports are available on fluorescent monoazo disperse dyes and the strategies to make them emissive [42–46]. Recently reported fluorescent dyes contained phenyl(1H-benzo[d]imidazol-5-yl)methanone as a core moiety [47]. So, we are interested to study the effect of incorporation of phenyl(1H-benzo[d]imidazol-5-yl)methanone moiety into few selected azo dyes available commercially. Moreover, as benzophenone core is well photostabilizing unit [17], it is expected that the designed dyes not only become red emission in nature but can also show good fastness properties.

In the present work, we are reporting three red emitting disperse dyes (**5a, 5b** and **5c)** containing in-built photostabilising and emission enhancing unit i.e. phenyl(1H-benzo[d]imidazol-5-yl)methanone. **5a, 5b** and **5c** disperse dyes exhibited red-shifted absorption and emission compared to corresponding parent analogues **CI Solvent Yellow 14 (5a') (CI 12055)**, **4-diethylamino-2-hydroxy-1-diazobenzene (5b')** and **7-(diethylamino)-4-hydroxy-3-(phenyldiazenyl)-2H-chromen-2-one) (5c')** dyes, respectively. Dye **5a** and its parent analogue dye **5a'** showed negative solvatochromism. Solvatochromic properties are in good agreement with solvent polarity graphs. Dyes **5a, 5b** and **5c** on dyed polyester and nylon showed excellent light and sublimation fastness compared to parent dyes **5a', 5b'** and **5c'** respectively.

Experimental Section

Materials and Methods

3,4-Diaminobenzophenone and *p*-nitrobenzaldehyde were procured by Spectrochem Pvt. Ltd. Mumbai.Naphthalen-2-oland were obtained from Sigma-Aldrich.3-(diethylamino)phenol, sodium nitrate, sodium carbonate, sodium hydroxide, conc. HCl, urea, metamol (dispersing agent), sodium chloride and all organic solvents were purchased from S. D. Fine Chemicals Ltd., Mumbai, India. All reagents and solvents were characterised by melting or boiling point and used without further purification. Readymade dyeing polyester (100%) substrate (weight70 gm/m^2) was purchased from Piyush Syndicate, Mumbai, India. Melting points were recorded on the instrument from Sunder Industrial Product, Mumbai. ^{1}H NMR and ^{13}C NMR spectra were recordedat 25 °C on Agilent NMR vnmrs 500 MHz and 125 MHz respectively. Chemical shifts were expressed in ppm using TMS as an internal standard. IR spectra were recorded on Perkin Elmer spectrum-100 FTIR spectrometer. Mass spectra were recorded on FINNIGAN LCQ ADVANTAGE MAX instrument from Thermo Electron Corporation (USA). All dying were performed on Flexi dyer machine (RossariLabtech, Mumbai, India).

Spectroscopic Instruments

Absorption and emission spectra of the compounds were recorded on Perkin Elmer Lambda 25 UV-Visible spectrophotometer and Varian Inc. Cary Eclipse spectrofluorometer respectively. 5 μM solutions of the dyes were prepared by using 7 different polarity solvents, viz. toluene, 1,4-dioxane, $CHCl_3$ (chloroform), EtOAc (ethyl acetate), MeOH (Methanol), acetonitrile and *N,N*-dimethylformamide (DMF).

Fastness and Color Assessment Instruments

Light fastness of dyed samples was tested on Q-Sun Xenon Test Chamber (Q-Lab Corporation, Ohio, USA) by the AATCC 16–2004 method. Sublimation fastness of the dyed samples were tested on Sublimation fastness tester (RBE Electronics Engg. Pvt. Ltd., Mumbai, India) by the standard method ISO 105-F04. Shade change and staining of adjacent fabrics were rated according to appropriate Society of Dyers & Colourists (SDC) grey scales**.** Colour properties of the dyed samples were measured using Spectra Scan 5100+ under the illuminant D65 using 10° standard observers.

Computational Study

All the DFT computations were performed using Gaussian 09 package [48] on an HP workstation XW 8600 with Xeon processor, 4 GB RAM and Windows Vista as the operating system. DFT and TD-DFT methods were employed for the ground state and excited state optimisations respectively. The hybrid functional B3LYP (Becke3-Lee-YangPar) as and 6-31G(d) basis set were used for all the atom [49]. Solvents used for Polarizable Continuum Model (PCM) [50] were toluene, 1,4-dioxane, chloroform ($CHCl_3$), ethyl acetate (EtOAc), methanol (MeOH), acetonitrile and *N,N*-dimethylformamide (DMF).

Synthesis and Characterization

Methanone (2-(4-nitrophenyl)-1H-benzo[d]imidazol-5-yl) phenyl (2)

Mixture of 3, 4 diaminobenzophenone **1** (1.09 g, 5.2 mmol), 4-nitrobenzaldehyde (0.71 g, 4.7 mmol) and water (25 mL) was taken in a round bottom flask. Potassium ferro-cyanide (0.17 g, 10 mol%) was added to the mixture and stirred at 30 °C for 2 h. Reaction was monitored by using TLC (thin layer chromatographic technique). After completion of the reaction, solid obtained was filtered, washed with water, dried and recrystallized from ethanol to obtain the desired product (Yield: 89%). Above said procedure and characterizations of compound **2** is reported in the literature [51].

Methanone(2-(4-aminophenyl)-1H-benzo[d]imidazol-5-yl) phenyl (3)

Compound **2** (2 g, 5.8 mmol) and Fe powder (0.81 g, 14.5 mmol) were added in the reaction-flask containing methanol (50 mL). To this mixture AcOH (0.83 mL, 14.5 mmol) was added slowly to keep temperature below 30 °C. The reaction mixture was then further refluxed at 64 °C for 30 min. Reaction was monitored by using thin layer chromatographic technique. After completion of the reaction, reaction mass was cooled and neutralized by using $NaHCO_3$. Precipitate formed was filtered, washed with water and dried. Recrystallization in EtOH afforded the desired product **3** (Yield: 70%). Above said procedure is reported in the literature [13]. Compound **3** is characterized and provided in supporting information.

Yield: 70%, Melting point: 196–199 °C.

^{1}H-NMR δ_H **(**500 MHz, DMSO, TMS**)**(ppm): 7.76 (2H, d, J = 8.0 Hz, Ar-H), 7.35 (2H, d, J = 8.0 Hz, Ar-H), 7.23 (2H, d, J = 7.5 Hz, Ar-H), 7.15 (2H, d, J = 7.5 Hz, Ar-H), 7.13 (1H, s, Ar-H), 7.05 (2H, t, J = 7.5 Hz, Ar-H), 6.99 (1H, d, J = 8.0 Hz, Ar-H), 5.52 (1H, s, N-H), 4.50 (2H, s, -NH_2).

^{13}C NMR δ_C **(**125 MHz, DMSO, TMS**)**(ppm): 196.51 (>C=O), 160.47 (-C=N), 153.63 (Ar-C-NH_2), 151.73 (Ar-C-NH), 139.09 (Ar-C-N=), 136.50 (Ar-C-CO), 134.00 (Ar-C), 133.05 (Ar-C-CO), 131.79 (Ar-C), 130.42 (Ar-C), 129.39 (Ar-C), 128.86 (Ar-C), 121.61 (Ar-C), 112.41 (Ar-C), 107.97 (Ar-C), 97.92 (Ar-C).

FT-IR: 3458 (N-H stretching), 1687 (C=O stretching), 1635 (Imine C=N stretch), 1281 (C-N stretching).

Mass (m/z): Calculated 314.12, $[M + H]^+$ for $C_{20}H_{16}N_3O^+$ found 314.1, $[M + H]^+$.

Elemental analysis (%) - Found: C, 76.6; H, 4.8; N, 13.4%; molecular formula $C_{20}H_{15}N_3O$ calculated: C, 76.66; H, 4.82; N, 13.41%.

General Procedure for Diazotization-Coupling Reactions

Mixture of amine **3** (3.3 mmol), conc. HCl (3 ml, 35.0 mmol), and water (15 mL) was boiled in reaction flask to get clear solution. Solution was then cooled to 0 °C followed by gradual addition of sodium nitrite (0.25 g, 3.6 mmol) with constant stirring. Solution was allowed to stir below 5 °C for 30 min and starch iodide paper was used as a process control test. Reaction was monitored by spot test. After completion of reaction urea was added to quench excess nitrous acid. Meanwhile, the couplers (3.3 mmol) were dissolved in 10% sodium hydroxide solution to get clear solution. Diazonium salt solution was gradually added to the respective coupler solutions with continuous stirring and maintaining the temperature below 5 °C. During addition of diazonium salt pH was maintained in between 7.5–8 using $NaCO_3$ (10% *w/v*) solution.

After completion of reaction precipitated was formed which was then filtered using a nutsche and washed thoroughly with water further. Recrystallized in ethanol afforded desired final dyes **5a**, **5b** and **5c** in good yields. Above said procedure is reported in literature [1].

Couplers used for coupling reactions were Naphthalen-2-ol, 3-(diethylamino)phenol and 7-(diethylamino)-4-hydroxy-2H-chromen-2-one. Synthetic scheme for the preparations of monoazo disperse dyes (**5a-5c)** is shown in Scheme 1**.** Structural analogues of **5a** is available in the literature [52]. 7-(diethylamino)-4-hydroxy-2H-chromen-2-one was prepared by reported procedure [45]. Dyes **5a' (CI Solvent Yellow 14**), **5b'** (4-diethylamino-2-hydroxy-1-diazobenzene) and **5c'** (7-(Diethylamino)-4-hydroxy-3-(phenyldiazenyl)-2H-chromen-2-one)) are available in the literature [45, 53–55]. Structural variations of present synthesised phenyl(1H-benzo[d]imidazol-5-yl)methanone based dyes are compared with previously reported parent dyes (Scheme 2**).**

Characterizations **(Supporting Information)**

5a:*Phenyl(2-phenyl 4-(2-hydroxynaphthalene-1-diazene)1H-benzo[d]imidazol-5-yl)methanone.*

Yield: 85%, Melting point: 129–131 °C.

^{1}H-NMR δ_H **(**500 MHz, DMSO, TMS**)** (ppm): δ13.40 (1H, s, Hydrogen bonding), 8.57 (1H, d, J = 8.5 Hz, Ar-H), 8.34 (2H, d, J = 8.5 Hz, Ar-H), 8.06–8.01 (2H, m, Ar-H), 7.97

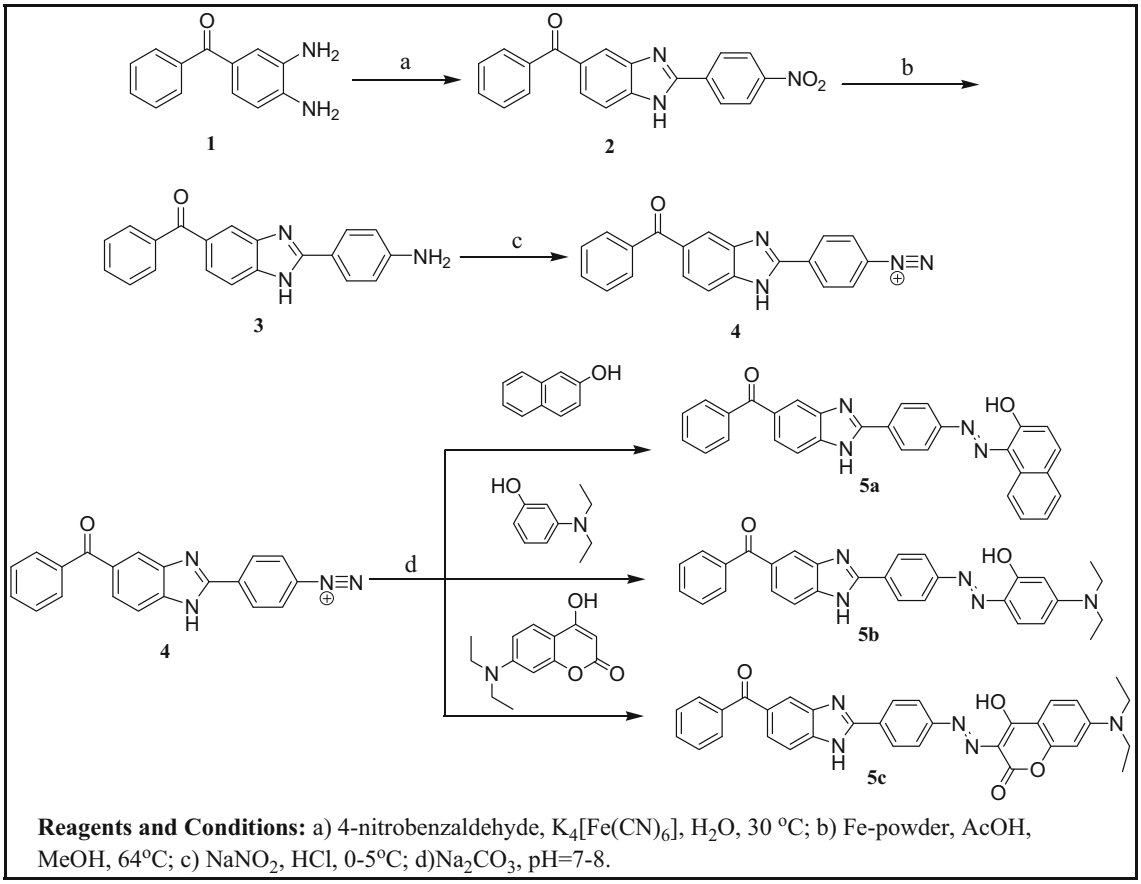

Scheme 1 Synthesis of monoazo disperse **5a**, **5b** and **5c** dyes

(1H, d, J = 9.5 Hz, Ar-H), 7.90 (1H, d, J = 4.0 Hz, Ar-H), 7.81 (1H, d, J = 8.5 Hz, Ar-H), 7.79–7.75 (2H, m, Ar-H), 7.70 (2H, dd, J = 12.0, 7.5 Hz, Ar-H), 7.64 (2H, dd, J = 15.5, 7.5 Hz, Ar-H), 7.58 (2H, t, J = 7.5 Hz, Ar-H), 7.48 (1H, t, J = 7.5 Hz, Ar-H), 6.88 (1H, dd, J = 9.5, 4.0 Hz, Ar-H), 5.48 (1H, s, N-H).

^{13}C NMR δ_C **(**125 MHz, DMSO, TMS**)**(ppm): 195.88 (>C=O), 156.02 (Ar-C-OH), 154.23 (-C=N), 153.34 (Ar-C-N=N), 147.75 (Ar-C-N=N), 146.02 (Ar-C-NH), 143.73 (Ar-C), 138.57 (Ar-C-NH), 135.14 (Ar-C), 134.77 (Ar-C), 133.50 (Ar-C), 133.15 (Ar-C), 132.53 (Ar-C), 131.65 (Ar-C), 131.50 (Ar-C), 130.39 (Ar-C), 129.88 (Ar-C), 128.88 (Ar-C), 128.78 (Ar-C), 128.66 (Ar-C), 128.45 (Ar-C), 126.91 (Ar-C), 125.16 (Ar-C), 122.16 (Ar-C), 119.34 (Ar-C), 114.60 (Ar-C), 111.96 (Ar-C), 109.98 (Ar-C), 106.98 (Ar-C), 100.13 (Ar-C).

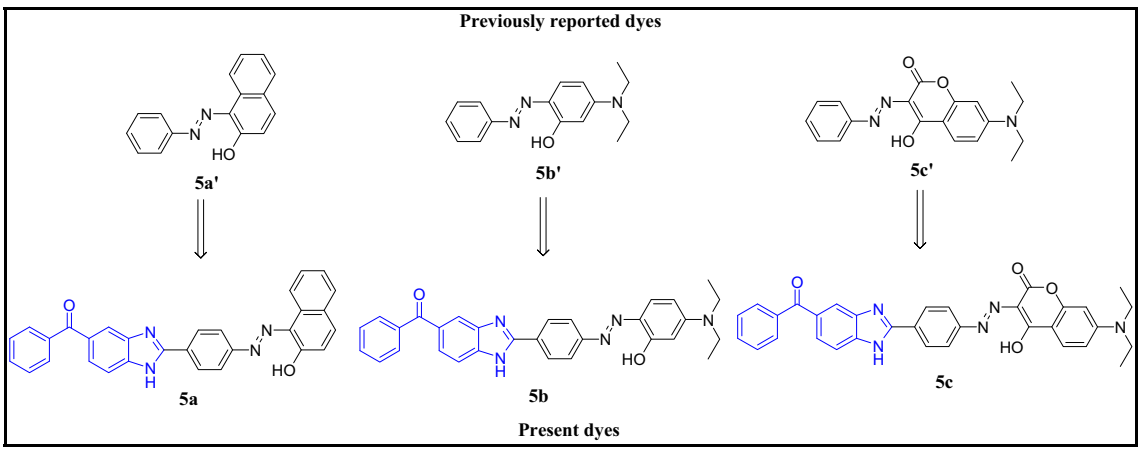

Scheme 2 Comparative structural variations of previously reported and present dyes

FT-IR: 3058 (O-H stretching phenolic), 1685 (C=O stretching), 1643 (C=C stretching), 1528 (N=N stretching), 1274 (C-N stretching) cm^{-1}.

Mass (m/z): Calculated 469.17, $[M+H]^+$ for $C_{30}H_{21}N_4O_2^+$ found 469.1, $[M+H]^+$.

Elemental analysis (%) - Found: C, 76.9; H, 4.3; N, 11.9%; molecular formula $C_{30}H_{20}N_4O_2$ calculated: C, 76.91; H, 4.30; N, 11.96%.

5b: Phenyl(2-phenyl 4-(3-(diethylamino)phenol)1H-benzo[d]imidazol-5-yl)methanone.

Yield: 71%, Melting point: 120–122 °C.

^{1}H-NMR δ_H **(**500 MHz, DMSO, TMS**)** (ppm): 13.33 (1H, s, Hydrogen bonding), 8.29 (2H, d, J = 8.5 Hz, Ar-H), 7.87 (3H, d, J = 8.5 Hz, Ar-H), 7.76 (2H, d, J = 7.5 Hz, Ar-H), 7.68 (2H, d, J = 7.5 Hz, Ar-H), 7.65 (1H, s, Ar-H), 7.58 (2H, d, J = 7.5 Hz, Ar-H), 7.56 (1H, s, Ar-H), 7.51 (1H, d, J = 9.0 Hz, Ar-H), 6.53 (1H, d, J = 9.0 Hz, Ar-H), 6.05 (1H, s, N-H), 3.46 (4H, q, J = 7.0 Hz, N-$(CH_2)_2$), 1.15 (6H, t, J = 7.0 Hz, N-(C-$CH_3)_2$).

^{13}C NMR δ_C **(**125 MHz, DMSO, TMS**)**(ppm): 195.98 (>C=O), 159.94 (Ar-C-N(Et)$_2$), 153.10 (Ar-C-OH), 151.20 23 (-C=N), 148.12 (Ar-C-N=N), 143.76 (Ar-C-N=N), 138.57 (Ar-C-NH), 135.97 (Ar-C), 133.47 (Ar-C-NH), 132.52 (Ar-C), 131.50 (Ar-C), 131.27 (Ar-C), 130.72 (Ar-C), 129.89 (Ar-C), 128.86 (Ar-C), 128.33 (Ar-C), 126.84 (Ar-C), 125.12 (Ar-C), 124.27 (Ar-C), 121.97 (Ar-C), 121.08 (Ar-C), 119.05 (Ar-C), 114.55 (Ar-C), 111.44 (Ar-C), 107.44 (Ar-C), 97.39 (Ar-C), 44.87 (N,N diethyl-CH_2), 13.18 (N,N diethyl-CH_3).

FT-IR: 3286 (N-H stretch imidazole), 2973 (O-H stretching phenolic).

1688 (C=O stretching), 1640 (C=C stretching), 1521 (N=N stretching), 1269 (C-N stretch) cm^{-1}.

Mass (m/z): Calculated 490.22, $[M+H]^+$ for $C_{30}H_{28}N_5O_2^+$ found 490.2, $[M+H]^+$.

Elemental analysis (%) - Found: C, 73.6; H, 5.5; N, 14.3%; molecular formula $C_{30}H_{27}N_5O_2$ calculated:C, 73.60; H, 5.56; N, 14.31%.

5c:Phenyl(2-phenyl4-(7-(diethylamino)-4-hydroxy-2H-chromen-2-one)1H-enzo[d]imidazol-5-yl)methanone.

Yield: 69%, Melting point: 139–142 °C.

^{1}H-NMR δ_H **(**500 MHz, DMSO, TMS**)** (ppm): 13.02 (1H, s, Hydrogen bonding), 7.98 (2H, d, J = 8.5 Hz, Ar-H), 7.56 (3H, d, J = 8.5 Hz, Ar-H), 7.45 (2H, d, J = 7.5 Hz, Ar-H), 7.36 (2H, d, J = 7.5 Hz, Ar-H), 7.34 (1H, s, Ar-H), 7.27 (2H, d, J = 7.5 Hz, Ar-H), 7.24 (1H, s, Ar-H), 7.20 (1H, d, J = 9.0 Hz, Ar-H), 6.22 (1H, d, J = 9.0 Hz, Ar-H), 5.74 (1H, s, N-H), 3.15 (4H, q, J = 7.0 Hz, N-$(CH_2)_2$), 0.84 (6H, t, J = 7.0 Hz, N-(C-$CH_3)_2$).

^{13}C NMR δ_C **(**125 MHz, DMSO, TMS**)**(ppm): 196.30 (>C=O), 160.26 (Ar-C-N(Et)$_2$), 157.37 (-CO-O), 153.42 (Ar-C-OH), 151.52 (-C=N), 148.44 (Ar-C-N=N), 144.08 (Ar-C-N=N), 138.89 (Ar-C-NH), 136.29 (Ar-C), 133.79 (Ar-C-NH), 132.84 (Ar-C), 131.81(Ar-C), 131.59 (Ar-C), 131.03 (Ar-C), 130.21 (Ar-C), 129.18 (Ar-C), 128.65 (Ar-C), 127.15 (Ar-C), 125.44 (Ar-C), 124.59 (Ar-C), 122.29 (Ar-C), 121.40 (Ar-C), 119.37 (Ar-C), 114.87 (Ar-C), 112.15 (Ar-C), 107.76 (Ar-C), 102.83 (Ar-C), 97.71 (Ar-C), 92.78 (Ar-C), 45.19 (N,N diethyl-CH_2), 13.49 (N,N diethyl-CH_3).

FT-IR: 3549 (N-H stretch imidazole), 3064 (O-H stretching phenolic), 1694 (C=O stretching), 1642 (C=C stretching), 1526 (N=N stretching), 1274 (C-N stretch) cm^{-1}.

Mass (m/z): Calculated 558.21, $[M+H]^+$ for $C_{33}H_{28}N_5O_4^+$ found 558.2, $[M+H]^+$.

Elemental analysis (%) - Found: C, 71.1; H, 4.8; N, 12.5%; molecular formula $C_{33}H_{27}N_5O_4$ calculated: C, 71.08; H, 4.88; N, 12.56%.

General Procedure of Dyeing

Nylon and polyester fabrics dyeing were carried out using 2% shade depth and material to liquor ratio of 1:30. Total dye solution calculated on the weight of fabric. As azo disperse dyes were insoluble in water, hence dissolved in 5 m*l* of N,N-dimethylformamide followed by dilution with 15 m*l* of buffered solution of pH 4 to 5 by using acetic acid in water. Ultrasonication for 30 min resulted in thefine dispersion of the dye in water. Saragen 50 was used as a dispersing agent. Nylon and polyester fabrics were dyed using the above dye solution. Dyeing was started at room temperature and raises to 130 °C (PET), 95 °C (Nylon) respectively temperatures for 50 min, and cooled to 60 °C**.** The dyed fabrics were rinsed with warm & cold water. Reduction clearing treatment was given only Polyester fabric using 2 g/l soda ash (Na_2CO_3), 2 g/l Sodium hydrosulphite and 1 g/l soap solution at 70 °C for 30 min (1:50) then treated fabrics were rinsed with cold water and allowed to dry in the open air.

Results and Discussion

Spectroscopic Characteristics

Absorption spectra of synthesised azo dyes were recorded in different polarity solvents (Fig. 1**)**. Tabulated results in Table 1 suggested that dye **5a** (λ_{max} = 504 nm to 516 nm) and its parent analogue **5a' (CI Solvent Yellow 14)** (λ_{max} = 472 nm to 476 nm) exhibited negative solvatochromism in absorption properties. On the other hand, dyes **5b** (λ_{max} = 498 nm to 513 nm) and **5c** (λ_{max} = 497 nm to 511 nm) and their respective parent analogues dyes **5b'** (λ_{max} = 364 nm to 376 nm) and **5c'** (λ_{max} = 456 nm to 460 nm) showed positive solvatochromism in absorption properties. Similarly, **5a, 5b** and **5c** on excitation from 497 nm to 516 nm exhibited significant solvatochromism in emission properties (Fig. 2**)**. Dye **5a** and is emitting with negative solvatochromism from 569 nm to 602 nm, while dyes **5b** and **5c** is emitting with positive

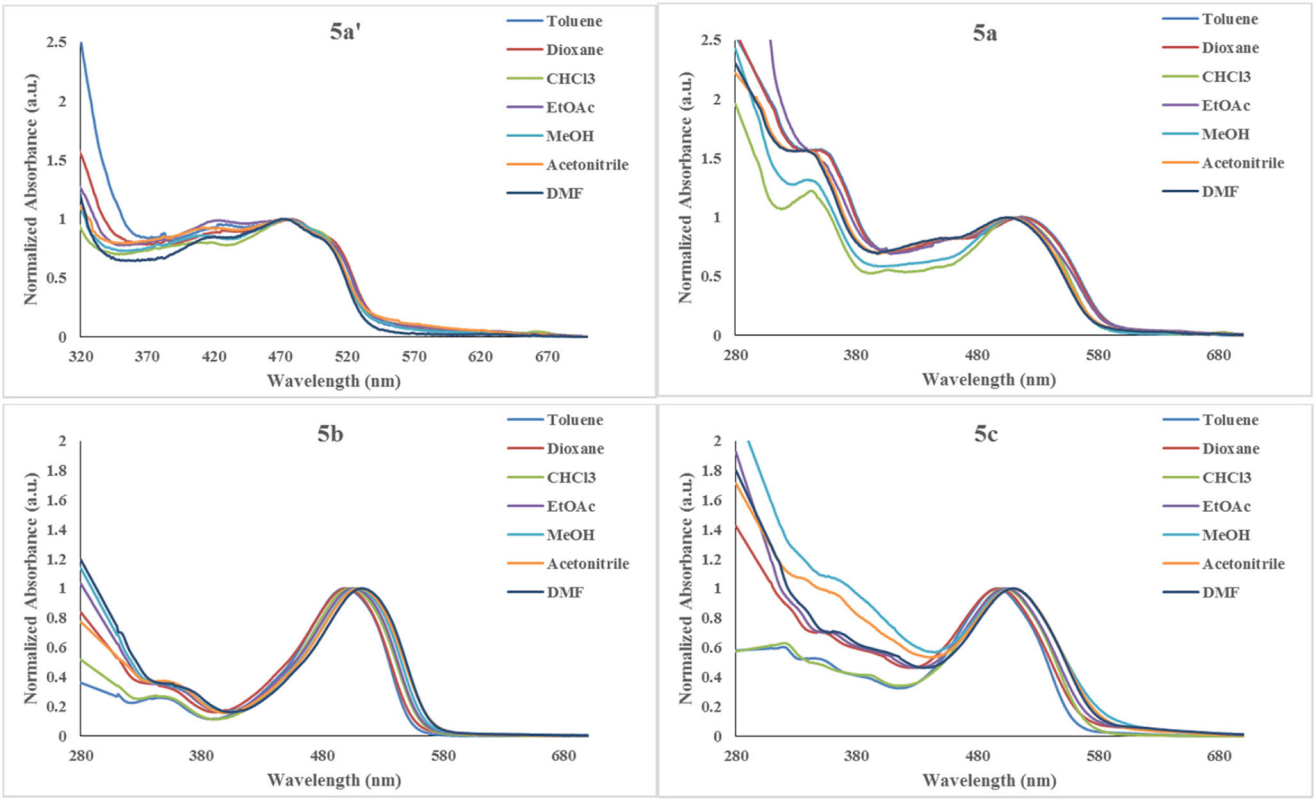

Fig. 1 Normalized Absorption spectra of **5a'**, **5a**, **5b** and 5c dyes in different solvent

solvatochromism from 565 nm to 627 nm in varying polarity solvents. **5a, 5b** and **5c** showed very high molar extinction coefficients (**ε**) as compared to parent dye **5a', 5b'** and **5c'**, respectively suggested increased in conjugation and the chromophore area.

Dyes **5a, 5b** and **5c** exhibited a small peak at around 340 nm which corresponds to the benzophenone unit. Stokes shift ($\Delta\vartheta$) of **5a** decreases from 2769 cm^{-1} (toluene) to 2267 cm^{-1} (DMF). On the other hand, Stokes shift ($\Delta\vartheta$) of **5b** and **5c** increases from 2444 cm^{-1} (toluene) to 2937 cm^{-1} (DMF) and from 2422 cm^{-1} (toluene) to 3621 cm^{-1} (DMF), respectively (Table 1**)**. All the synthesised dyes have a significant effect of solvent polarity on Stokes shifts ($\boldsymbol{\Delta\vartheta}$). **5a** exhibited minimum $\boldsymbol{\Delta\vartheta}$ in DMF (2267 cm^{-1}) while maximum in toluene (2769 cm^{-1}). On contrary, **5b** and **5c** exhibited minimum $\boldsymbol{\Delta\vartheta}$ in toluene (2444 cm^{-1}) and (2422 cm^{-1}) while maximum $\boldsymbol{\Delta\vartheta}$ in DMF (2927 cm^{-1}) and (3621 cm^{-1}) respectively.

Among all the parent dyes, only **5c'** is weakly emissive in nature and show positive solvatochromism. The dye **5c'** exhibited significantly larger Stokes shifts having minimum $\boldsymbol{\Delta\vartheta}$ in toluene (3377 cm^{-1}) while maximum in acetonitrile (5662 cm^{-1}) (Table 1**)**. Hence, it can be concluded that significant effect of substituents on spectroscopic characteristics of the dyes have been observed.

It is reported that tautomer forms of monoazo dyes in equilibrium can be shifted towards hydrazone form by treating these dyes with acid titrations [56]. Further it is also described that azo bridge get protonated in acidic medium resulted into formation of azonium cation [57]. So in order to get into the details of possible forms of the dyes, trifluoroacetic acid (acid) was added to dyes solutions (in methanol) resulting into a new strong red shifted absorption band in absorption spectra at around 582 nm to 592 nm region (Supporting Information **Fig. S1 (a)**). In the acidic medium highly expected protonated azonium cation is formed [57].

Stability study was performed under Ultraviolet irradiation (at 254 nm) for better understanding of stabilities of azo and protonated forms of the dyes. Stabilities studies of protonated forms carried out at pH = 3 (in methanol) suggested that protonated forms of **5b** and **5c** are stable under irradiations. Azo forms of **5a**, **5b** and **5c** dyes are also found to be stable under ultraviolet irradiation (Supporting Information **Fig. S1 (b)**).

Estimations of Photo-Physical Properties

The role of solvent polarity and different substituents for altering spectroscopic processes have been estimated in terms of the radiative rate constant ($\mathbf{k_r}$), then on-radiative rate constant ($\mathbf{k_{nr}}$) and life time $\boldsymbol{\tau}$ (ns) evaluations. Relative fluorescence quantum yields ($\boldsymbol{\Phi_f}$) of **5a, 5b** and **5c** were obtained by using Rhodamine 6G ($\boldsymbol{\Phi_f = 0.94}$ in Ethanol) as standard. $\mathbf{k_{nr} >> k_r}$ for all dyes indicate so much loss of energy during non-radiative processes. $\mathbf{k_r}$ are found to be in good agreement with

Table 1 Spectroscopic characteristics of **5a, 5b**, **5c, 5a', 5b'** and **5c'** dyes in different solvents

Dye	Entry	Toluene	Dioxane	CHCl3	EtOAc	MeOH	Acetonitrile	DMF
5a'	λ_{max} (nm)	476	476	475	474	473	473	472
	ε (mM^{-1} cm^{-1})	7.4	9.2	9.8	9.6	10.4	10.2	7.6
5a	λ_{max} (nm)	516	515	513	510	507	506	504
	ε (mM^{-1} cm^{-1})	8.8	15.0	12.1	12.0	14.2	12.8	8.4
	λ_{emm} (nm)	602	599	593	587	579	576	569
	$\Delta\vartheta$ (nm)	86	84	80	77	72	70	65
	$\Delta\vartheta$ (cm^{-1})	2769	2723	2630	2572	2453	2402	2267
5b'	λ_{max} (nm)	364	366	367	370	372	373	376
	ε (mM^{-1} cm^{-1})	9.4	9.1	9.0	9.5	8.9	9.3	9.6
5b	λ_{max} (nm)	498	500	503	506	509	510	513
	ε (mM^{-1} cm^{-1})	24.0	29.0	27.0	27.0	32.0	29.0	22.0
	λ_{emm} (nm)	567	571	577	585	594	597	604
	$\Delta\vartheta$ (nm)	69	71	74	79	85	87	91
	$\Delta\vartheta$ (cm^{-1})	2444	2487	2550	2669	2811	2857	2937
5c'	λ_{max} (nm)	456	457	453	457	463	460	460
	ε (mM^{-1} cm^{-1})	9.9	10.9	9.8	9.5	10.2	10.1	10.4
	λ_{emm} (nm)	539	581	588	582	613	622	621
	$\Delta\vartheta$ (nm)	83	124	135	125	150	162	161
	$\Delta\vartheta$ (cm^{-1})	3377	4670	5068	4700	5285	5662	5636
5c	λ_{max} (nm)	497	499	502	505	508	509	511
	ε (mM^{-1} cm^{-1})	22.0	30.0	23.0	24.0	12.0	15.0	19.0
	λ_{emm} (nm)	565	570	586	594	605	616	627
	$\Delta\vartheta$ (nm)	68	71	84	89	97	107	116
	$\Delta\vartheta$ (cm^{-1})	2422	2496	2855	2967	3156	3413	3621

low fluorescence quantum yield ($\mathbf{\Phi_f}$). Life time ($\boldsymbol{\tau}$) has not shown significant variations with the varying polarity of the solvents (Table 2).

Solvent Polarity Graphs

Statistical evalution for solvatochromic properties of **5a**, **5b** and **5c** is provided by solvent polarity functions like Lippert-Mataga, Weller and Bhakshiev. Lippert-Mataga plot [58] has shown very good linearity of Stokes shift vs. $f_{LM(\varepsilon,\eta)}$ functions with excellent regression coefficients ($R^2 \geq 0.9834$) suggested a significant effect of solvent polarity on Stokes shift. Stokes shift decreases for **5a**, while increases for **5b** and **5c** with increasing solvent polarity (Fig. 3a). Weller's equation allows estimation of the excited state dipole moments [59] and gave the plot of emission frequency (cm^{-1}) versus Weller's function [60]. Weller plot showed distinct positive slope with excellent regression coefficients ($R^2 = 0.9853$) for **5a** indicated negative solvatochromism. On the other hand, anegative slope with excellent regression coefficients of $R^2 = 0.9868$ and $R^2 \geq 0.9960$ for **5b** and **5c** indicated positive solvatochromism (Fig. 3b). Not only Stokes shift and emission properties were affected by solvent polarity, but also absorption is also sensitive to the solvent polarity. So we utilised Bakhshiev plot which depends on additive frequencies of absorption and emission with solvent polarity functions [60]. Bakhshiev plot showed significant positive slope for dyes **5a** ($R^2 = 0.9939$), and significant negative slope for dyes **5b** ($R^2 = 0.9940$) and **5c** ($R^2 = 0.9958$) (Fig. 3c). Hence we can reveal that significant effect of naphthalene and *N,N*-diethylamine substituents were observed, resulting into negative solvatochromism for dye **5a** in both absorption and emission while opposite trend of positive solvatochromism was observed for **5b** and **5c** in both absorption and emission.

Colour Properties of the Dyes

Dyes **5a, 5b**, **5c, 5a', 5b'**and **5c'**were applied at 2% shade with MLR 1:30 on nylon and polyester respectively. Dyeing was evaluated using the CIELAB system in terms of L^*, a^* and b^*.

K/S values were determined by using below eq. 1 [61].

$$\frac{K}{S} = \frac{(1-R)^2}{2R} \quad (1)$$

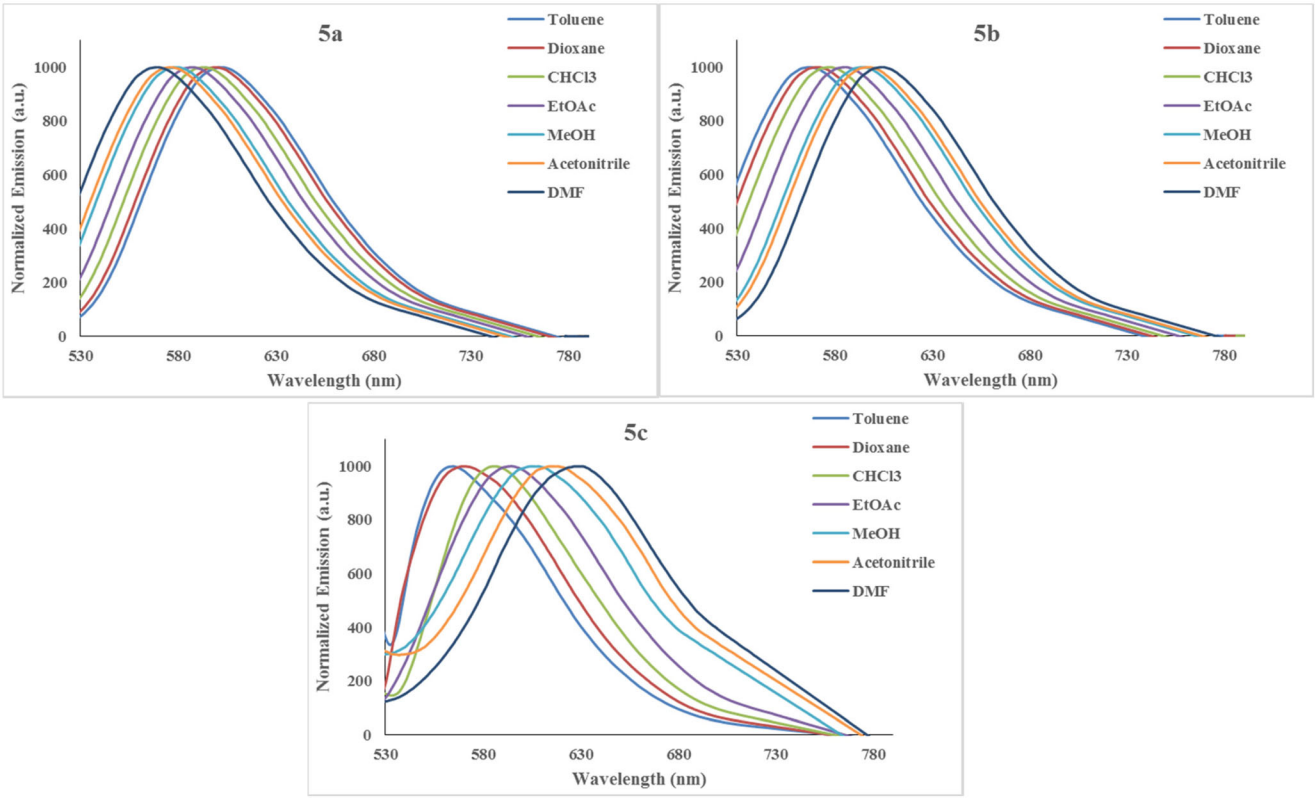

Fig. 2 Normalised Emission spectra of dyes **5a** (excited at 504–516 nm), **5b** (excited at 498–513 nm) and **5c** (excited at 497–511 nm) in different solvents

where, R is the reflectance of coloured samples and K and S are the absorption and scattering coefficients respectively.

Comparative K/S values of Dyes all the dyes dyed on nylon are tabulated in Table 3**. 5c** showed highest K/S compared to other dyes due to presence of presence of extended conjugated fluorescent coumarin core. Phenyl(1H-benzo[d]imidazol-5-yl)methanone based **5a**, **5b** and **5c** dyes have good colour strengths compared to respective parent analogues **5a'**, **5b'**

Table 2 Estimated spectroscopic (emission) characteristics of **5a, 5b**, **5c** and **5c'** in different solvent

Dye	Entry	Toluene	Dioxane	CHCl3	EtOAc	MeOH	Acetonitrile	DMF
5a	Φ_f	0.0127	0.0211	0.0101	0.0184	0.0173	0.0176	0.0149
	τ (ns)	0.12	0.13	0.12	0.13	0.14	0.13	0.15
	Kr (s-1)	1.0×10^8	1.6×10^8	0.8×10^8	1.4×10^8	1.2×10^8	1.3×10^8	1.0×10^8
	$K_{nr}(s^{-1})$	8.1×10^9	7.8×10^9	8.3×10^9	7.6×10^9	7.2×10^9	7.4×10^9	6.6×10^9
5b	Φ_f	0.0183	0.0367	0.0219	0.0288	0.0321	0.0214	0.0177
	τ (ns)	0.09	0.13	0.09	0.12	0.12	0.09	0.09
	K_r (s^{-1})	2.0×10^8	2.9×10^8	2.3×10^8	2.5×10^8	2.8×10^8	2.3×10^8	2.0×10^8
	$K_{nr}(s^{-1})$	1.1×10^{10}	0.7×10^{10}	1.0×10^{10}	0.8×10^{10}	0.8×10^{10}	1.0×10^{10}	1.2×10^{10}
5c'	Φ_f	0.0094	0.0108	0.0131	0.0157	0.0011	0.0028	0.0024
	τ (ns)	0.11	0.14	0.10	0.09	0.12	0.14	0.14
	K_r (s^{-1})	1.8×10^8	2.1×10^8	1.6×10^8	1.4×10^8	1.7×10^8	1.2×10^8	2.5×10^8
	$K_{nr}(s^{-1})$	8.1×10^9	7.6×10^9	8.6×10^9	7.8×10^9	8.4×10^9	8.1×10^9	7.1×10^9
5c	Φ_f	0.0367	0.0501	0.0346	0.0411	0.0239	0.0278	0.0339
	τ (ns)	0.13	0.11	0.13	0.12	0.13	0.13	0.14
	K_r (s^{-1})	2.7×10^8	4.7×10^8	2.6×10^8	3.4×10^8	1.9×10^8	2.1×10^8	2.5×10^8
	$K_{nr}(s^{-1})$	7.2×10^9	8.9×10^9	7.3×10^9	8.0×10^9	7.6×10^9	7.3×10^9	7.1×10^9

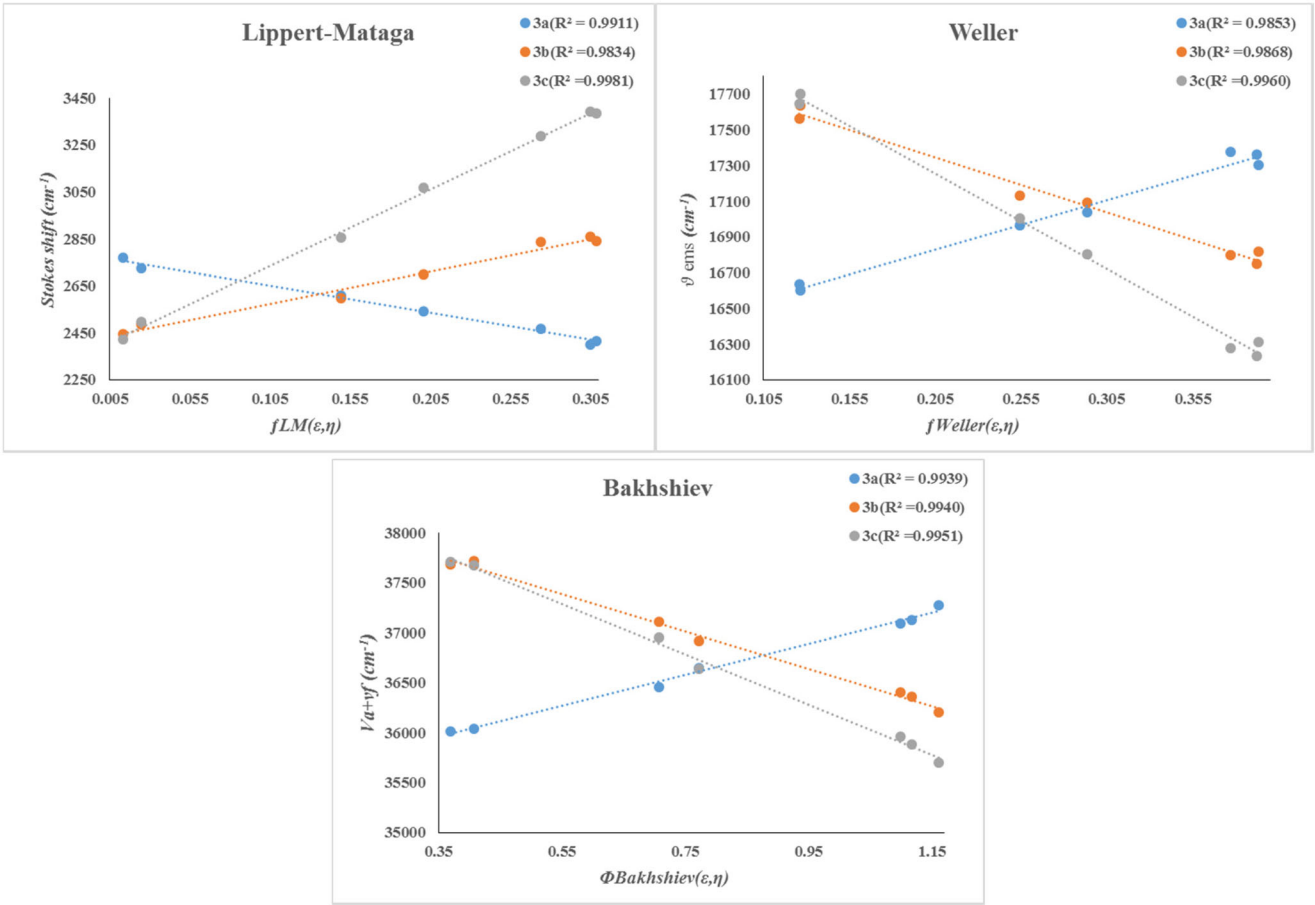

Fig. 3 Solvent polarity plots: **a** Lippert-Mataga, **b** Weller plot and **c** Bakhshiev plot of **5a**, **5b** and **5c** dyes for different polarity solvents

and **5c'**. Good K/S strength of a dyeing and higher values of present dyes represent darker and more saturated colours.

Comparative K/S values of all the dyes dyed on polyester are tabulated in Table 4**. 5a** showed highest K/S compared to other dyes due to presence of presence of extended conjugated fluorescent coumarin core. Dyes **5a, 5b** and **5c** are having higher K/S values compared to their respective analogues **5a'**, **5b'** and **5c'**. Good K/S strength of a dyeing and higher values of present dyes represent darker and more saturated colours.

Light Fastness Properties

Evaluations of light fastness properties of dyes were performed by comparative light fastness measurements of before and after exposure of dyed polyester and nylon samples to the xenon lamp. Same dyed sample was used for measurement in order to have more precision and better comparison of light fastness values. Half part of the sample was exposed to a xenon lamp for 48 h while the other half was covered during the light fastness determination. The samples were then

Table 3 Color coordinates (CIELAB) of **5a, 5b**, **5c, 5a', 5b'** and **5c'** dyes for Nylon dyeing

Dye	L*	a*	b*	c*	h^0	K/S
5a'	41.1	38.9	39.5	55.4	45.4	19.06
5a	31.2	26.3	18.4	32.1	34.9	27.61
5b'	39.2	33.9	37.8	52.5	42.3	13.87
5b	41.1	16.9	45.6	48.7	69.6	22.56
5c'	43.1	41.5	44.4	56.7	49.3	24.06
5c	57.9	35.1	65.7	74.5	61.8	36.60

Table 4 Color coordinates (CIELAB) of **5a, 5b**, **5c, 5a', 5b'** and **5c'** dyes for Polyester dyeing

Dye	L*	a*	b*	c*	h^0	K/S
5a'	57.9	46.0	76.6	89.4	58.9	32.65
5a	41.2	54.5	43.7	69.9	38.6	52.59
5b'	53.8	47.2	73.7	89.6	57.9	29.95
5b	41.3	46.8	41.5	62.6	41.6	44.69
5c'	49.9	43.3	70.8	85.7	55.8	26.82
5c	43.1	44.7	49.7	66.9	48.0	39.09

compared with the Blue wool standard scale and fastness ratings were given. On comparing light fastness values of dyed polyester and dyed nylon for any dye, it can be concluded that dyed polyester sample have slightly better light fastness compared to dyed nylon sample. Moreover, light fastness of all the synthesized dyes (**5a**, **5b** and **5c)** varies from good to very good for dyed polyester and dyed nylon samples (Table 5**)**. It can be further concluded that synthesized dyes showed better light fastness as compared to commercially available respective analogues **5a'**, **5b'** and **5c'** dyes.

Sublimation Fastness

In order to get the sublimation fastness, dyed samples were sandwiched between two undyed cloth pieces (cotton and polyester/nylon) and were subjected to 150 °C, 180 °C and 210 °C for 30 s in a sublimation fastness tester. Two parameters, i.e. colour change (cc) and colour staining (on undyed cloth) [cs] were rated. Synthesized dyes **5a**, **5b** and **5c** showed better sublimation fastness as compared to previously available **5a'**, **5b'** and **5c'** derivative at all the temperatures (Table 5) on polyester and nylon. Dyes **5a**, **5b** and **5c** exhibited excellent sublimation fastness for (150 °C, 180 °C, 210 °C) on both polyester and nylon.

DFT Study

Geometry Optimisation and Calculated Energies of Tautomer Forms

There is a possibility of the existence of tautomer forms that is evident from shoulder peaks in the absorption spectra of these dyes (Fig. 1). Optimised structures of Azo and Hydrazone forms of dyes **5a** at B3LYP/6-31G(d) in chloroform have shown in supporting information **Fig. S2**. It is clearly observed that both the forms have a significant difference at the 47H atom. An azo form of **CI Solvent Yellow 14 (5a')** and **5a** are stable than the corresponding hydrazone forms. On the other hand hydrazone forms of **5b** and **5c** are stable than azo forms (Table 6).

Frontier Molecular Orbital Energies

Energy levels of frontier molecular orbitals i.e. HOMO, LUMO and their spatial distributions can give insight into excitation properties and the idea of the ability of hole or electron injection, which in turn allowed to understand photostability and spectroscopic characteristics of the dyes. In order to get into the stability details of azo and hydrazone forms of the dyes, comparative energy levels and electronic densities need to study. Pictorial diagram of FMO's suggested that the electron densities at HOMOs of **CI Solvent Yellow 14** (**5a'**) and **5a** dyes were located on the N=N motif, while electron densities on the LUMOs were found to be localised on N=N motif periphery of the azo forms of the dyes (Fig. 4a**)**. On the other hand, electron densities at HOMOs of **5b** and **5c** dyes were located on *N,N*-diethylamino, -N=N- and imidazole motif. Electron densities at the LUMOs were found to be localised mostly on the >C=O motif of the azo forms of the dyes. This suggested that there is good charge transfer was observed in **5b** and **5c** dyes resulting into significant positive solvatochromism. HOMO-LUMO energy gap is significantly reduced in **5a** compared to **CI Solvent Yellow 14**. Moreover, there is lowering of HOMO and LUMO energy levels of **5a** compared to **CI Solvent Yellow 14** clearly suggested red-shifted absorption maxima in **5a.** Dyes **5b** and **5c** are also having similar energy levels as compared to **5a**. So, improved spectroscopic characteristics were observed for dyes **5a**, **5b** and **5c** compared to **5a'** dye.

HOMO-LUMO electronic densities of hydrazone forms of **5a'** and **5a** showed truncated delocalization of electronic densities compared to corresponding azo forms of dyes (Fig. 4b**)**. Moreover, HOMO energy levels of azo forms of **5a'** and **5a** are more stabilized than hydrazone forms. On the other hand, HOMO and LUMO electronic densities of hydrazone forms

Table 5 Light and sublimation fastness ratings of **5a, 5b**, **5c, 5a', 5b'** and **5c'** dyes for dyed nylon and polyester

Dye	Polyester				Nylon			
	Light fastness rating	Sublimation fastness rating			Light fastness rating	Sublimation fastness rating		
	(1–8)*	(1–5)*			(1–8)*	(1–5)*		
		150 °C	180 °C	210 °C		150 °C	180 °C	210 °C
5a'(Solvent Yellow 14)	5/6	3	2/3	2	5	2/3	2	1/2
5a	7	4/5	4	3/4	6/7	4	3/4	3
5b'	6	2/3	2	1/2	5/6	3	2/3	2
5b	7	4/5	4	3/4	6/7	4	3/4	3
5c'	6	2/3	2/3	2	5	3	2/3	2
5c	7	4/5	4	3/4	6/7	4	3/4	3/4

Table 6 Comparative energies of azo and hydrazone forms of **5a'**, **5a, 5b** and **5c** dyes in Chloroform at B3LYP/6-31G(d)

Compound name	E/Hartree	ΔE/kJ mol-1	ΔG/Hartree
5a'Azo	−801.388745	0	−801.440571
5a'Hydrazone	−801.384091	12.221404	−801.445106
5a Azo	−1524.261226	0	−1524.345413
5a Hydrazone	−1524.256309	12.912042	−1524.35064
5b Azo	−1583.128132	0.845572	−1583.22673
5b Hydrazone	−1583.128454	0	−1583.227169
5c Azo	−1847.882662	28.221622	−1847.988914
5c Hydrazone	−1847.893409	0	−1848.000234

of **5b** and **5c** dyes are comparatively same as that of their azo forms, but HOMO energy levels of hydrazone forms are more stabilized than their corresponding azo (Fig. 4b**)**.

Calculated HOMO and LUMO energy levels for the azo forms of dyes in solvents of varying polarity suggested that there were an increase in the energy gap for dyes **5a** (2.850 to 2.880 eV) and **CI Solvent Yellow 14 (5a')** (3.723 to 3.752 eV) with increasing solvent polarity, correlated with negative solvatochromism. On the other hand, **5b** (2.729 to 2.704 eV) and **5c** (2.766 to 2.745 eV) showed decrease in the energy gap with increase in the solvent polarities correlated with the positive solvatochromism (Supporting Information **Fig. S3a**). Similar trends were observed for hydrazone forms of the dyes. **5a'** and **5a** dyes showed slight elevation of HOMO energy levels while **5b** and **5c** showed lowering of HOMO levels

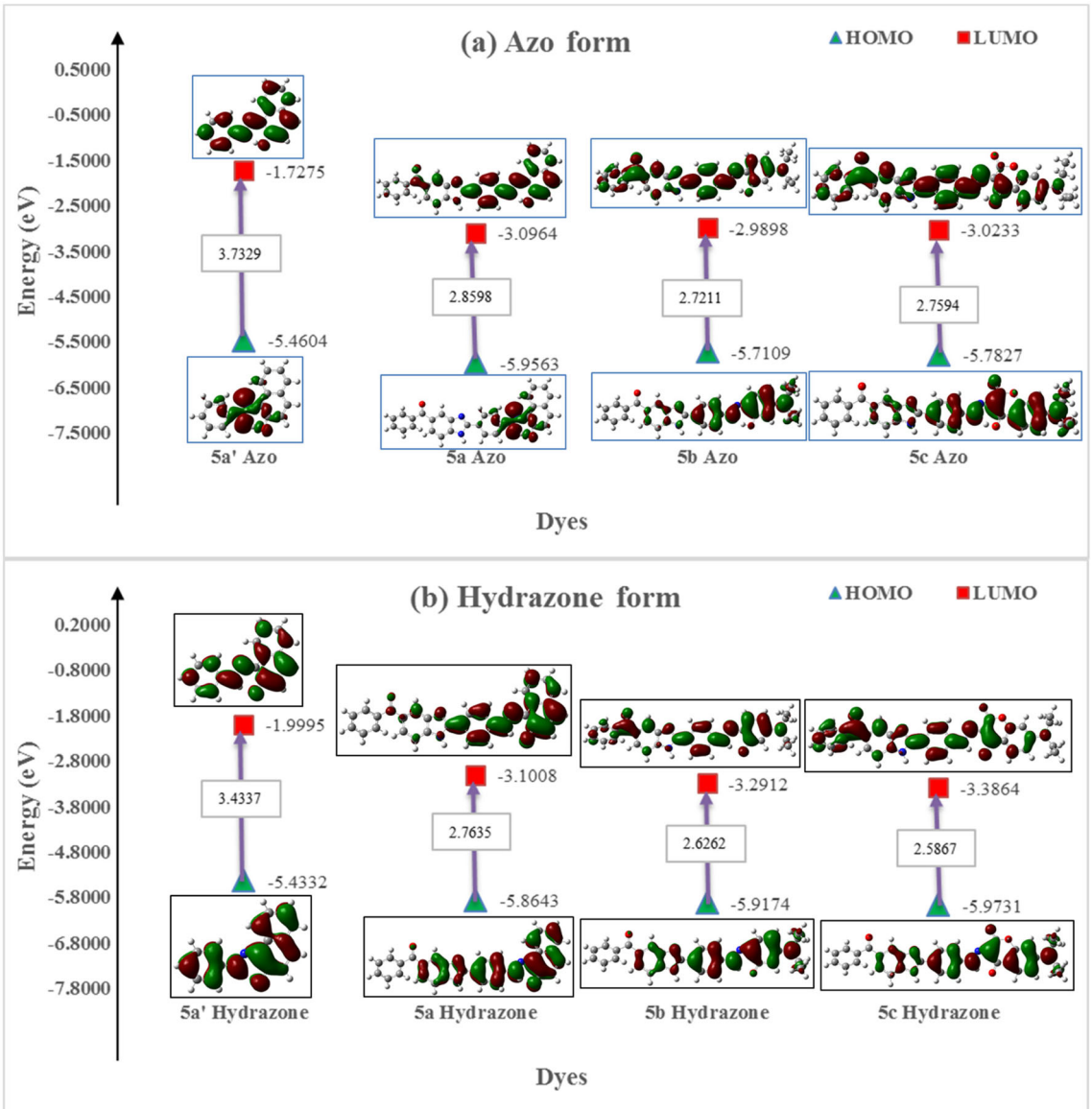

Fig. 4 **(a)** Comparative molecular orbitals and energy gaps of azo forms of **5a'**, **5a, 5b** and **5c** dyes optimized at B3LYP/6-31G(d) in chloroform **(b)** Comparative molecular orbitals and energy gaps of hydrazone forms of **5a'**, **5a, 5b** and **5c** dyes optimised at B3LYP/6-31G(d) in chloroform

compared to their corresponding azo forms. LUMO energy levels and HOMO-LUMO band gap is lowered in all the hydrazone forms of the dyes compared to their corresponding azo forms (Supporting Information **Fig. S3b**).

TD-DFT

Ground state optimised geometry of dyes at ground state in solvents of various polarities was subjected to TD using B3LYP/6-31G(d) function. At least 10 excited states were calculated for each molecule. Comparative absorption maxima, computed vertical excitations, oscillator strength and their orbital contributions in chloroform are listed in Table 7. The results of DFT and TD-DFT suggest that there was the observable influence of (1H-benzo[d]imidazol-5-yl)(phenyl)methanone group on the absorption spectra of the dyes. Computed values for these dyes are in good agreement with the experimental observations.

Electrophilicity Index

We have calculated the stability of the dyes mathematically using computationally deduced energies at B3LYP/6-31G(d). For this reason, the electrophilicity index (ω) was utilised. As defined by Parr et al. [62, 63], this electrophilicity index measures the propensity of the moiety to absorb electrons and is mathematically formulated as:

$$\omega = \frac{\mu^2}{2\eta} \tag{2}$$

where,

ω electrophilicity index
μ chemical potential
η chemical hardness

$$\mu = -\frac{(IP + EA)}{2} \tag{3}$$

$$\eta = \frac{(IP - EA)}{2} \tag{4}$$

where, *IP* = Ionization Potential, i.e., the change in the energy when an electron is removed from the system.

EA = Electron Affinity, i.e., the change in the energy when an electron is added to the system

$$\mu = \frac{(E_{LUMO} + E_{HOMO})}{2} \tag{5}$$

$$\eta = \frac{(E_{LUMO} - E_{HOMO})}{2} \tag{6}$$

Table 7 Comparison of experimental data and computed data at B3LYP/6-31G(d) for **5a'**, **5a, 5b** and **5c** dyes in chloroform

Experimental					Theoretical (TD-DFT)			
Compound	λ_{max} [a] (nm)	Molar Absorptivity ($dm^3\ mol^{-1}\ cm^{-1}$)	*f*[a]	μge (Debye)	Vertical[b] excitation (nm)	Band gap (eV)	*f*[b]	Orbital contribution
5a'	475	120,000	0.2153	4.05	474	2.61570	0.2826	H → L (98%)
5a	513	96,000	0.1111	3.44	510	2.43106	0.1254	H → L (99%)
5b	503	270,000	0.1118	3.17	501	2.47473	0.1533	H → L (98%)
5c	502	230,000	0.1299	9.11	499	2.48465	0.1967	H → L (99%)

[a] Experimentally obtained
[b] Theoretically calculated

Table 8 Electrophilicity index of azo and hydrazone forms of **5a'**, **5a, 5b** and **5c** dyes optimized at B3LYP/6-31G(d) in chloroform

Dyes	E(kJ mol-1)	HOMO	LUMO	Difference	Sum	μ	η	ω	ω^-	ω^+	$\omega^{\pm}$
5a'Azo	−801.646260	−0.22075	−0.06351	0.15724	−0.28426	−0.14213	0.07862	0.128472	0.0038312	0.0003171	0.0041483
5a'Hydrazone	−801.640841	−0.21895	−0.10936	0.10959	−0.32831	−0.164155	0.054795	0.24588798	0.0026268	0.0006553	0.0032821
5a Azo	−1524.721459	−0.21898	−0.11384	0.10514	−0.33282	−0.16641	0.05257	0.2633849	0.0025208	0.0006813	0.0032021
5a Hydrazone	−1524.715793	−0.21686	−0.11509	0.10177	−0.33195	−0.165975	0.050885	0.27068587	0.002393	0.000674	0.003067
5b Azo	−1583.676130	−0.20446	−0.10022	0.10424	−0.30468	−0.15234	0.05212	0.22263503	0.0021788	0.0005235	0.0027023
5b Hydrazone	−1583.676870	−0.21155	−0.10357	0.10798	−0.31512	−0.15756	0.05399	0.22990511	0.0024162	0.0005791	0.0029954
5c Azo	−1848.460555	−0.2126	−0.11115	0.10145	−0.32375	−0.161875	0.050725	0.25828995	0.0022927	0.0006267	0.0029194
5c Hydrazone	−1848.472662	−0.21593	−0.11272	0.10321	−0.32865	−0.164325	0.051605	0.26162877	0.0024061	0.0006557	0.0030618

All symbols have their usual meanings

where,E_{LUMO} is the energy of the lowest unoccupied molecular orbital and E_{HOMO} is the energy of the highest occupied molecular orbital.

$$\omega^{\pm} = \omega^{+} + \omega^{-} \tag{7}$$

where,

$$\omega^{+} = \frac{(E_{LUMO})^2}{2(E_{LUMO} - E_{HOMO})} \tag{8}$$

and

$$\omega^{-} = \frac{(E_{HOMO})^2}{2(E_{LUMO} - E_{HOMO})} \tag{9}$$

Among azo and hydrazone forms of the dyes the stable conformation of dyes were justified by calculating net electrophilicity index ($\omega^{\pm}$) [1]. The net electrophilicity index ($\omega^{\pm}$) allowed us to predict comparative stabilities of azo and hydrazone tautomer forms of the dyes. Net electrophilicity index ($\omega^{\pm}$) suggested that azo form of **5a'** and **5a** dye are slightly more stable than hydrazone forms. On the other hand, the exactly reverse trend was observed for **5b** and **5c** dyes with hydrazone forms were slightly more stable than azo forms (Table 8).

Conclusion

Three novel phenyl(1H-benzoimidazol-5-yl)methanone based fluorescent monoazo disperse dyes were successfully synthesised. The dyes **5a, 5b** and **5c** exhibited red-shifted absorption maxima from 497 nm to 516 nm and much higher molar extinction coefficient as compared to compared to parent dyes **5a', 5b'** and **5c'** respectively**.** The dyes **5a, 5b** and **5c** are emitting in the far-red region (565–627 nm) while only **5c'** is weakly emitting (539 to 621 nm). Dye **5a** and **5a'** showed negative solvatochromism, while dyes **5b, 5c, 5b'** and **5c'** showed positive solvatochromism. Solvent polarity graphs are in good agreement with solvatochromic data. Dyes **5a, 5b** and **5c** on dyed polyester and nylon showed very good light and sublimation fastness. DFT calculated energies, electrophilicity index and Frontier Molecular Orbitals calculations of **5a, 5b** and **5c** are in good agreements with the experimental observations. **5a, 5b** and **5c** are emission in nature and has good fastness properties on fabrics, so can find the potential applications in high-visibility colour dyeing of textile products [64].

Acknowledgements One of the author Amol G. Jadhav is thankful to UGC for financial assistance in terms of SRF.

Suvidha Shinde is thankful to the Centre of Advanced Studies (UGC) for JRF and SRF under the Special Assistance Programme (SAP).

References

1. Bhide R, Jadhav AG, Sekar N (2016) Light fast monoazo dyes with an inbuilt photostabilizing unit: Synthesis and computational studies. Fibers Polym 17:349–357. https://doi.org/10.1007/s12221-016-5717-3
2. Sharma RK, Gulati S, Pandey A, Adholeya A (2012) Novel, efficient and recyclable silica based organic–inorganic hybrid Nickel catalyst for degradation of dye pollutants in a newly designed chemical reactor. Appl Catal B Environ 125:247–258. https://doi.org/10.1016/j.apcatb.2012.05.046
3. Sekar N (2014) Natural colorants versus synthetic colorants. Colourage 61:54–56
4. Bafana A, Devi SSCT (2011) Azo dyes: past, present and the future. Environ Rev 19:350–370
5. Seesuriyachan P, Takenaka S, Kuntiya A et al (2007) Metabolism of azo dyes by Lactobacillus casei TISTR 1500 and effects of various factors on decolorization. Water Res 41:985–992. https://doi.org/10.1016/j.watres.2006.12.001
6. Al-Sheikh M, Medrasi HY, Usef Sadek K, Mekheimer RA (2014) Synthesis and Spectroscopic Properties of New Azo Dyes Derived from 3-Ethylthio-5-cyanomethyl-4-phenyl-1,2,4-triazole. Molecules 19:2993–3003. https://doi.org/10.3390/molecules19032993
7. Abdou MM (2013) Thiophene-Based Azo Dyes and Their Applications in Dyes. Chemistry 3:126–135. https://doi.org/10.5923/j.chemistry.20130305.02.
8. Athalye A (2015) Automotive Textiles. Int J Text Eng Process 1:42–52
9. Ravve A (2006) Photosensitizers and Photoinitiators. In: Light React Synth Polym. Springer New York, New York, pp 23–122
10. Jiang X, Rui Y, Chen G (2009) Improved Properties of Cotton by Atmospheric Pressure Plasma Polymerization Deposition of Sericin. J Vinyl Addit Technol 21:129–133. https://doi.org/10.1002/vnl
11. Patel HM (2014) Synthesis, Structure Investigation and Dyeing Assessment of Novel Bisazo Disperse Dyes Derived from UV Absorbing Material. IOSR. J Appl Chem 6:51–55
12. Bochet CG (2014) 9.13 Organic Photochemistry. In: Compr Org Synth II. Elsevier, pp 330–350
13. Jadhav AG, Shinde SS, Lanke SK, Sekar N (2017) Benzophenone based fluorophore for selective detection of Sn2+ ion: Experimental and theoretical study. Spectrochim Acta Part A Mol Biomol Spectrosc 174:291–296. https://doi.org/10.1016/j.saa.2016.11.051
14. Dorman G, Prestwich GD (1994) Benzophenone Photophores in Biochemistry. Biochemistry 33:5661–5673. https://doi.org/10.1021/bi00185a001
15. Sen GA, Paul K, Luxami V (2015) Ratiometric fluorescent chemosensor for fluoride ion based on inhibition of excited state intramolecular proton transfer. Spectrochim Acta, Part A Mol Biomol Spectrosc 138:67–72. https://doi.org/10.1016/j.saa.2014.11.026
16. Sen GA, Paul K, Luxami V (2016) Benzimidazole based ratiometric chemosensor for detection of CN− and Cu2+ ions in protic/aqueous system: Elaboration as XOR logic operation. Inorganica Chim Acta 443:57–63. https://doi.org/10.1016/j.ica.2015.11.024
17. Kiguchi M, Evans PD (1998) Photostabilisation of wood surfaces using a grafted benzophenone UV absorber. Polym Degrad Stab 61:33–45. https://doi.org/10.1016/S0141-3910(97)00124-9
18. Chou P-T, Chen Y-C, Yu W-S et al (2001) Excited-State Intramolecular Proton Transfer in 10-Hydroxybenzo[h]quinoline. J Phys Chem A 105:1731–1740. https://doi.org/10.1021/jp002942w
19. Mitchell D, Lukeman M, Lehnherr D, Wan P (2005) Formal Intramolecular Photoredox Chemistry of Meta-Substituted Benzophenones. Org Lett 7:3387–3389. https://doi.org/10.1021/ol051381u
20. Beckett A, Porter G (1963) Primary photochemical processes in aromatic molecules. Part 10.-Photochemistry of substituted benzophenones. Trans Faraday Soc 59:2051. https://doi.org/10.1039/tf9635902051
21. Dixit B, Patel H, Dixit R, Desai D (2010) Synthesis, characterization and dyeing assessment of novel acid azo dyes and mordent acid azo dyes based on 2- hydroxy-4-methoxybenzophenone on wool and silk fabrics. J Serbian Chem Soc 75:605–614. https://doi.org/10.2298/JSC090704039D
22. Tsatsaroni EG, Eleftheriadis IC (2004) UV-absorbers in the dyeing of polyester with disperse dyes. Dyes Pigments 61:141–147. https://doi.org/10.1016/j.dyepig.2003.10.002
23. Barsotti F, Brigante M, Sarakha M et al (2015) Photochemical processes induced by the irradiation of 4-hydroxybenzophenone in different solvents. Photochem Photobiol Sci 14:2087–2096. https://doi.org/10.1039/c5pp00214a
24. Bhasikuttan a C, Singh a K, Palit DK et al (1998) Laser Flash Photolysis Studies on the Monohydroxy Derivatives of Benzophenone. Laser Flash Photolysis Studies on the Monohydroxy Derivatives of Benzophenone J Phys Chem 102:3470–3480. https://doi.org/10.1021/jp972375l
25. Das PK, Encinas MV, Scaiano JC (1981) Laser flash photolysis study of the reactions of carbonyl triplets with phenols and photochemistry of p-hydroxypropiophenone. J Am Chem Soc 103:4154–4162. https://doi.org/10.1021/ja00404a029
26. Palit DK (2005) Photophysics and excited state relaxation dynamics of p-hydroxy and p-amino-substituted benzophenones: a review. Res Chem Intermed 31:205–225. https://doi.org/10.1163/1568567053147020
27. Barsotti F, Ghigo G, Berto S, Vione D (2017) The nature of the light absorption and emission transitions of 4-hydroxybenzophenone in different solvents. A combined computational and experimental study. Photochem Photobiol Sci. https://doi.org/10.1039/C6PP00272B
28. Kumar D, Justin Thomas KR, Lee C, Ho K (2014) Organic Dyes Containing Fluorene Decorated with Imidazole Units for Dye-Sensitized Solar Cells. J Org Chem 79:3159–3172. https://doi.org/10.1021/jo500330r
29. Aulakh RK, Sandhu S, Tanvi, et al (2015) Designing and synthesis of imidazole based hole transporting material for solid state dye sensitized solar cells. Synth Met 205:92–97. doi: https://doi.org/10.1016/j.synthmet.2015.03.030
30. Skonieczny K, Ciuciu AI, Nichols EM et al (2012) Bright, emission tunable fluorescent dyes based on imidazole and π-expanded imidazole. J Mater Chem. https://doi.org/10.1039/c2jm33891b
31. Zhang X, Chen Y (2013) Synthesis and fluorescence of dicyanoisophorone derivatives. Dyes Pigments 99:531–536. https://doi.org/10.1016/j.dyepig.2013.05.031
32. Li W, Lin W, Wang J, Guan X (2013) Phenanthro[9,10- d]imidazole-quinoline Boron Difluoride Dyes with Solid-State Red Fluorescence. Org Lett 15:1768–1771. https://doi.org/10.1021/ol400605x
33. Prostota Y, Kachkovsky OD, Reis LV, Santos PF (2013) New unsymmetrical squaraine dyes derived from imidazo[1,5-a]pyridine. Dyes Pigments 96:554–562. https://doi.org/10.1016/j.dyepig.2012.10.006
34. Fouassier J, Allonas X, Burget D (2003) Photopolymerization reactions under visible lights: principle, mechanisms and examples of applications. Prog Org Coatings 47:16–36. https://doi.org/10.1016/S0300-9440(03)00011-0
35. Wan Z, Zhou L, Jia C et al (2014) Comparative study on photovoltaic properties of imidazole-based dyes containing varying electron

acceptors in dye-sensitized solar cells. Synth Met 196:193–198. https://doi.org/10.1016/j.synthmet.2014.08.005
36. Tsai M, Hsu Y-C, Lin JT et al (2007) Organic Dyes Containing 1 H -Phenanthro[9,10- d]imidazole Conjugation for Solar Cells. J Phys Chem C 111:18785–18793. https://doi.org/10.1021/jp075653h
37. Shank NI, Zanotti KJ, Lanni F et al (2009) Enhanced Photostability of Genetically Encodable Fluoromodules Based on Fluorogenic Cyanine Dyes and a Promiscuous Protein Partner. J Am Chem Soc 131:12960–12969. https://doi.org/10.1021/ja9016864
38. Bamfield P, Britain) RS of C (Great (2001) Chapter 3. Phenomena Involving Absorption of Energy Followed by Emission of Light. In: Chromic Phenom. Royal Society of Chemistry, Cambridge, pp 234–365
39. Szuster L, Kaźmierska M, Król I (2004) Fluorescent dyes destined for dyeing high-visibility polyester textile products. Fibres Text East Eur 12:70–75
40. Youssef BM, Ahmed MHM, Arief MMH, Mashaly HM (2014) Synthesis and Application of Functional (Anti-UV) Azo-dyes based on γ -acid on Wool Fabrics. Indian J Sci Technol 7:1005–1013
41. Kano N, Yamamura M, Kawashima T (2015) 2,2′-Disilylazobenzenes Featuring Double Intramolecular Nitrogen···Silicon Coordination: A Photoisomerizable Fluorophore. Dalt Trans 44:16256–16265. https://doi.org/10.1039/C5DT02038G
42. Satam MA, Raut RK, Sekar N (2013) Fluorescent azo disperse dyes from 3-(1,3-benzothiazol-2-yl)naphthalen-2-ol and comparison with 2-naphthol analogs. Dyes Pigments 96:92–103. https://doi.org/10.1016/j.dyepig.2012.07.019
43. Yoshino J, Kano N, Kawashima T (2013) Fluorescent azobenzenes and aromatic aldimines featuring an N–B interaction. Dalt Trans 42:15826. https://doi.org/10.1039/c3dt51689j
44. Deshmukh MS, Sekar N (2015) Chemiluminescence properties of isoluminol related mono azo disperse dyes: Experimental and DFT based approach to photophysical properties. Dyes Pigments 115:127–134. https://doi.org/10.1016/j.dyepig.2014.12.019
45. Tathe AB, Sekar N (2016) Red Emitting Coumarin—Azo Dyes : Synthesis, Characterization, Linear and Non-linear Optical Properties-Experimental and Computational Approach. J Fluoresc 26:1279–1293. https://doi.org/10.1007/s10895-016-1815-2
46. Warde U, Sekar N (2017) NLOphoric mono-azo dyes with negative solvatochromism and in-built ESIPT unit from ethyl 1,3-dihydroxy-2-naphthoate: Estimation of excited state dipole moment and pH study. Dyes Pigments 137:384–394. https://doi.org/10.1016/j.dyepig.2016.10.032
47. Jadhav AG, Sekar N (2017) Substituent Modulation from ESIPT to ICT Emission in Benzoimidazolphenyl-methanones Derivatives: Synthesis, Photophysical and DFT Study. J Solut Chem 46:777–797. https://doi.org/10.1007/s10953-017-0602-2
48. Frisch MJ, Trucks GW, Schlegel HB, et al (2009) Gaussian 09, Revision C.01. Gaussian 09, Revis B01, Gaussian, Inc, Wallingford CT
49. Becke AD (1988) Density-functional exchange-energy approximation with correct asymptotic behavior. Phys Rev A 38:3098–3100. https://doi.org/10.1103/PhysRevA.38.3098
50. Zhao Y, Truhlar DG (2008) The M06 suite of density functionals for main group thermochemistry, thermochemical kinetics, noncovalent interactions, excited states, and transition elements: two new functionals and systematic testing of four M06-class functionals and 12 other function. Theor Chem Accounts 120:215–241. https://doi.org/10.1007/s00214-007-0310-x
51. Shaikh KA, Patil VA, Shaikh PA (2012) An Efficient and Convenient Synthesis of Imidazolines and Benzimidazoles via Oxidation of Carbon-Nitrogen Bond in Water Media. Chinese J Chem 30:924–928. https://doi.org/10.1002/cjoc.201100210
52. Devi TC, Krishnan R, Kunju AS (2004) Synthesis and Characterization of Copper(II), Cobalt(II) and Manganese(II) Complexes of 2-(2′-hydroxynaphthylazo)-5-benzoulbenzimidazole. Asian J Chem 16:1611–1617
53. Munro CH, Smith WE, Armstrong DR, White PC (1995) Assignments and Mechanism of SERRS of the Hydrazone Form for the Azo Dye Solvent Yellow 14. J Phys Chem 99:879–885. https://doi.org/10.1021/j100003a008
54. Olson DH, Camblor MA, Villaescusa LA, Kuehl GH (2004) Light hydrocarbon sorption properties of pure silica Si-CHA and ITQ-3 and high silica ZSM-58. Microporous Mesoporous Mater 67:27–33. https://doi.org/10.1016/j.micromeso.2003.09.025
55. Maximilian Paul Schmidt W-B, and Hermann Neuroth, Wiesbaden G (1934) LIGHT-SENSITIVE LAYER. 3–4.
56. Chen X-C, Tao T, Wang Y-G et al (2012) Azo-hydrazone tautomerism observed from UV-vis spectra by pH control and metal-ion complexation for two heterocyclic disperse yellow dyes. Dalt Trans 41:11107. https://doi.org/10.1039/c2dt31102j
57. Peters AT (1995) Freeman HS. Modern Colorants, Synthesis and Structure. https://doi.org/10.1007/978-94-011-1356-4
58. Lanke SK, Sekar N (2016) Aggregation induced emissive carbazole-based push pull NLOphores: Synthesis, photophysical properties and DFT studies. Dyes Pigments 124:82–92. https://doi.org/10.1016/j.dyepig.2015.09.013
59. Leu WCW, Fritz AE, Digianantonio KM, Hartley CS (2012) Push-pull macrocycles: Donor-acceptor compounds with paired linearly conjugated or cross-conjugated pathways. J Org Chem 77:2285–2298. https://doi.org/10.1021/jo2026004
60. Tathe AB, Sekar N (2016) Red-emitting NLOphoric carbazole-coumarin hybrids - Synthesis, photophysical properties and DFT studies. Dyes Pigments 129:174–185. https://doi.org/10.1016/j.dyepig.2016.02.026
61. Mashaly HM, Abdelghaffar RA, Kamel MM, Youssef BM (2014) Dyeing of Polyester Fabric using Nano Disperse Dyes and Improving their Light Fastness using ZnO Nano Powder. Indian J Sci Technol 7:960–967
62. Parr RG, Szentpály LV, Liu S (1999) Electrophilicity index. J Am Chem Soc 121:1922–1924. https://doi.org/10.1021/ja983494x
63. Gupta VD, Tathe AB, Padalkar VS et al (2013) Red emitting solid state fluorescent triphenylamine dyes: Synthesis, photo-physical property and DFT study. Dyes Pigments 97:429–439. https://doi.org/10.1016/j.dyepig.2012.12.024
64. Hamdaoui M, Lanouar A, Halaoua S (2015) Study of Fluorescent Dyeing Process and Influence of Mixture Dyes on High-visibility. J Eng Fiber Fabr 10:89–96